Simulation of Vibrational Spectra of Acetic Acid By an Extended Molecular Mechanics Method and Half Band Width Parameters

Isao YOKOYAMA, Yoshihisa MIWA, and Katsunosuke MACHIDA*
Faculty of Pharmaceutical Sciences, Kyoto University, Yoshida, Sakyo-ku, Kyoto 606
(Received November 20, 1991)

The molecular mechanics simulation of the infrared absorption and Raman spectra of acetic acid in the solution or liquid phase has been carried out by using an empirically estimated force field which includes the equilibrium charges and the charge fluxes as the Coulomb potential parameters. The variation of the observed band widths among different normal modes has been taken into account by introducing the half band width parameters empirically assigned to individual internal coordinates. The half widths of more than 20 bands observed in the infrared absorption and the Raman spectra are well reproduced in terms of five half band width parameters. The thermodynamic properties and the structures of acetic acid monomer and dimer are successfully simulated. The overall features of the simulated spectra of acetic acid are in good agreement with the observed ones.

Carboxylic acids in both the gas and the condensed phases tend to form a hydrogen-bonded centrosymmetric cyclic dimer, which causes mutually exclusive infrared absorption (u-type antisymmetric) and Raman (g-type symmetric) bands. In the infrared absorption spectrum, the OH stretching band exhibits marked changes of all the three spectral characteristics, the frequency, the intensity, and the band width, on the dimerization. These are the low-frequency shift by about 500 cm^{-1}, the intensification by a factor of about 15, and the considerable band broadening.[1-3]

In our previous works,[4] calculations of the thermodynamic quantities, the structure parameters, and the infrared absorption and Raman spectra of formic acid monomer and dimer were carried out by using an extended molecular mechanics method. An OH stretching charge flux, $\partial q_{OH}/\partial r_{OH}$, was introduced to elucidate the frequency shift and intensification of the infrared absorption band due to the OH stretching mode on the dimerization. The large splitting between the A_g and the B_u carbonyl stretching frequencies and extension of the dimeric carbonyl bond as compared to the monomer were explained in terms of two carbonyl stretching charge fluxes, $\partial q_{C=O}/\partial r_{C=O}$ and $\partial q_{O\cdots H}/\partial r_{C=O}$. Furthermore, Raman spectral simulation of formic acid in the gas phase was successfully carried out.

In this work, infrared absorption spectra in the carbon tetrachloride solution and Raman spectra in the liquid phase of acetic acid are simluated by using an empirical force field which includes the equilibrium charges and the charge fluxes as Coulomb potential parameters. The Raman intensity parameters of acetic acid have been empirically estimated on the basis of the bond polarizability model. The broad band widths of the OH stretching and the OH out-of-phane deformation modes, as compared with the other bands in the infrared absorption spectra, were reproduced by introducing empirical half band width parameters for the related internal coordinates.

Calculation

Potential Parameters. The potential parameters related to the carboxyl group were taken from formic acid,[4] and those related to the methyl group from *n*-alkanes,[5] and the iterative improvement of each parameter was carried out in order for achieving closer fit of related experimental data. The data of longer *n*-fatty acids were also referred to when necessary, as mentioned below for individual cases. As in the previous works, the potential function is written in the form:

$$V=\sum_i D_i \exp\{-a_i(r_i-r_i^0)\}[\exp\{-a_i(r_i-r_i^0)\}-2]$$
$$+(1/2)\sum_i\sum_j F_{ij}(R_i-R_i^0)(R_j-R_j^0)$$
$$+(1/2)\sum_n\sum_i V_{ni}\{1-(-1)^n\cos n\tau_{ni}\}$$
$$+(1/2)\sum_i\sum_j V_{NB}(r_{ij})+(1/2)\sum_i\sum_j q_i q_j(1/\varepsilon_{ij}r_{ij}). \quad (1)$$

Among the Morse parameters in the first sum in Eq. 1, all the intrinsic bond lengths, r_i^0, were fixed at the transferred values,[4] while the intrinsic dissociation energies D_i for the C–C_α and H–C_α bonds were slightly modified to fit the heats of formation of acetic through heptanoic acids.[6] For the OH bond in the dimer, D_i should be increased a little from the transferred value in order to give the larger heat of dimerization of acetic acid[7] than formic acid.[8] The parameters α in the same term as those revised D_i's were then adjusted to reproduce the relevent vibrational frequencies. An alternative way of fitting the heat of dimerization is to adjust the Morse parameters of the hydrogen bond O···H, but this choice fails to give reasonable frequencies of the hydrogen-bond stretching modes. In a preliminary calculation, the Morse parameters of the OH bond determined for acetic acid were confirmed to be transferable to higher fatty acids.

In the second sum representing a general valence-type quadratic potential, the intrinsic values R_i^0 of the C_α–C–

O and C_α–C=O angles were so chosen as to reproduce the observed angles[9,10] of the monomer and the dimer separately. The general valence-type force constants related to the junction of the methyl and the carboxyl groups of the dimer were taken initially from the force field by Kishida and Nakamoto.[11] These constants were refined, together with the other valence force constants, to fit the observed frequencies in infrared absorption and Raman spectra[12] in the solution or in the liquid phase under the influence of the other potential terms. In the case of the monomer, the force constants concerning the carboxyl and the methyl groups were taken from formic acid monomer and acetic acid dimer, respectively. Though much ambiguity still remains for the assignments of the monomer frequencies,[13–16] we have found no obvious reason for adjusting the transferred force constants except for F_{ii}(O–C=O), F_{ii}(C_α–C–O), F_{ij}(C–O, C–O–H), and F_{ij}(C–O–H, O–C=O), which are all related to the carboxyl group.

In the internal rotation potential terms around the

Table 1. Potential Parameters

Bond stretching

r_i		α_i/Å^{-1}	D_i/aJ	r_i^0/Å	r_i		α_i/Å^{-1}	D_i/aJ	r_i^0/Å
H–C_α		1.7974	0.7278	1.095*	C=O	(monomer)	2.0840	1.3500*	1.190*
H–O	(monomer)	2.1401*	0.7755*	1.000*		(dimer)	2.1100	1.3500*	1.190*
	(dimer)	2.2010	0.7927	1.000*	H···O	(dimer)	1.5500*	0.0480*	1.670*
C–C_α		2.1090	0.5640	1.500					
C–O	(monomer)	2.2423*	0.6010*	1.330*					
	(dimer)	2.5410	0.6010*	1.330*					

Intrinsic angles and general quadratic force constants (Diagonal)

θ_i		θ_i^0/deg	F_{ii}/aJ rad^{-2}	θ_i		θ_i^0/deg	F_{ii}/aJ rad^{-2}
H–C_α–H		109.5*	0.4950	C–O–H	(monomer)	102.5*	0.5515*
H–C_α–C		109.5*	0.6432		(dimer)	107.0*	0.7915
C_α–C–O	(monomer)	109.5	0.8000	O–H···O	(dimer)		
	(dimer)	112.0	0.5519		(in-plane)	0.0*	0.0050*
C_α–C=O	(monomer)	124.5	1.2226		(out-of-plane)	0.0*	0.1150
	(dimer)	122.0	1.2226	C=O···H		120.0*	0.0400*
O–C=O	(monomer)	126.0*	0.5200	CO_2 out-of-plane		0.0*	0.3850
	(dimer)	126.0*	0.9800				

General quadratic force constants (Off-diagonal)

Symbol	F_{ij}	Symbol	F_{ij}
Stretching–Stretching/N cm^{-1}		Stretching–Bending/10^{-8} N rad^{-1}	
H–C_α, C_α–C	0.1191	H–O–C, C–O	−0.2500 (monomer)
C_α–C, C–O	0.4344		−0.0104 (dimer)
C_α–C, C=O	0.0258	O–C=O, C–O	0.3849 (monomer)*
C–O, O–H	0.4067 (monomer)*		0.4522 (dimer)
	0.1271 (dimer)	O–C=O, C=O	0.0111 (monomer)*
O–C, C=O	0.2916 (monomer)*		0.4856 (dimer)
	0.4626 (dimer)		
Stretching–Bending/10^{-8} N rad^{-1}		Bending–Bending/aJ rad^{-2}	
H–C_α–H, H–C_α	0.2790	H–C_α–H, H–C_α–C	0.0352
H–C_α–C, H–C_α	0.5552	H–C_α–C, H–C_α–C	−0.0300
H–C_α–C, C_α–C	0.1204	C_α–C–O, C_α–C=O	−0.1637
C_α–C=O, C_α–C	0.8092	O–C=O, C_α–C=O	−0.1138
C_α–C=O, C=O	−0.0286	H–C_α–C, C_α–C–O	$-0.1173C_\tau$[a]
C_α–C–O, C–C_α	0.4008	H–C_α–C, C_α–C=O	$0.0764C_\tau$[b]
C_α–C–O, C–O	0.4267	C_α–C–O, C–O–H	−0.2200
H–O–C, O–H	0.0369 (monomer)*	H–O–C, O–C=O	−0.1500 (monomer)
	0.0728 (dimer)		−0.2450 (dimer)
Torsion potential parameters/10^{-2} aJ			
V_{3i}(H–C_α–C–O)	3.580×10^{-2}	V_{2i}(O=C–O–H)	4.440 (monomer)*
V_{3i}(H–C_α–C=O)	-3.580×10^{-2}		2.100 (dimer)*
V_{2i}(C_α–C–O–H)	4.440 (monomer)	V_{2i}(C_α–C=O···H)	0.800 (dimer)
	3.800 (dimer)	V_{2i}(O–C=O···H)	0.600 (dimer)*

a) The dependance on the dihedral angle H–C_α–C–O is introduced by using a factor $C_\tau=\cos\tau_{H\text{-}C_\alpha\text{-}C\text{-}O}$. b) The dependance on the dihedral angle H–C_α–C=O is introduced by using a factor $C_\tau=\cos\tau_{H\text{-}C_\alpha\text{-}C=O}$. The symbol * denotes the transferred value from formic acid or *n*-alkane.

skeletal bond in the third term, the two-fold torsional parameters for the C_α–C–O–H and C_α–C=O···H were newly estimated from the observed fundamental frequencies[17,18] below 200 cm^{-1}. As each conformation in which a hydrogen atom of the methyl group eclipses the carbonyl group corresponds to an energy minimum in acetic acid,[9] the signs of the three-fold torsional parameters for the H–C_α–C–O and the H–C_α–C=O angles should be positive and negative, respectively. The absolute values of these two parameters of the monomer were assumed to be equal, and were determined from the observed rotational barrier with respect to the C–C_α bond, 2.01 kJ mol^{-1},[19] by microwave spectra. This value reproduces the $CH_3(CD_3)$ torsional frequencies[15] of the monomer as well. The potential parameters in the first through the third sums of Eq. 1 are summarized in Table 1.

The form and the parameter values for the exchange repulsion-dispersion potential[4,5] in the fourth sum are the same as those for formic acid.[4] The last sum represents the Coulomb potential between effective atomic charges, q_i, which are approximated as linear functions of internal coordinates in the form:

$$q_i = q_i^0 + \sum_p (R_p - R_p^0) \sum_k \left(\frac{\partial q_{ki}}{\partial R_p} \right), \qquad (2)$$

where q_i^0 is the ith intrinsic atomic charge and $\partial q_{ki}/\partial R_p$ represents the bond charge flux from atom k to atom i associated with the unit increase of the internal coordinate R_p. The intrinsic atomic charge was calculated from the Pauling electronegativities,[20] χ_i, and the bond charge parameters β_{ki} and γ_{li} according to Eq. 3:

$$q_i^0 = \sum_k \beta_{ki}(\chi_k - \chi_i) + \sum_l \gamma_{li}. \qquad (3)$$

So far, we have used only the first sum in Eq. 3 in the expression of q_i^0,[4,5] but this term cannot represent any charge flow through a bond r_{li}, for which χ_l and χ_i are equal to each other. The C–C_α bond of acetic acid belongs to this type of homogeneous bonds as far as the Pauling electronegativities[20] are used. The newly introduced second sum in Eq. 3 involves the correction terms for such a case, where γ_{li} denotes the charge flow from the atom l to the atom i of the bond r_{li} consisting of the same element. We have already used such an auxiliary charge flow through the C_α–C_β bond of n-alkyl ether.[5] The parameters β_{ki} and γ_{li}, which we shall call the heterogeneous and the homogeneous bond charge parameters, respectively, may be taken to specify the zeroth- and the first-order terms of the power series expansion of the charge flow with the difference in the electronegativities between the two end atoms. The

Table 2. Bond Charge Parameters and Bond Charge Fluxes in Acetic Acid Monomer and Dimer

Bond charge parameters		Angle bending fluxes[b]/e rad^{-1}	
Heterogeneous β/e[a]		CH_3C group[c]	
H–C_α	0.1500	$\partial q_{C_\alpha H}/\partial \theta_{HC_\alpha H}$	−0.005
C–O	0.0193*	$\partial q_{C_\alpha H}/\partial \theta'_{HC_\alpha H}$	−0.015
C=O	0.3187*	$\partial q_{C_\alpha H}/\partial \theta_{HC_\alpha C}$	−0.015
O–H	0.2390 (monomer)*	$\partial q_{C_\alpha H}/\partial \theta'_{HC_\alpha C}$	0.020
	0.1300 (dimer)*	$\partial q_{C_\alpha C}/\partial \theta_{HC_\alpha C}$	−0.004
Homogeneous γ/e[a]		$\partial q_{C_\alpha C}/\partial \theta'_{HC_\alpha H}$	0.004
C–C_α	0.1380	CO_2 group[d]	
Bond stretching fluxes[b]/e $Å^{-1}$		$\partial q_{C=O}/\partial \theta_{O-C=O}$	0.130
$\partial q_{C_\alpha H}/\partial r_{HC_\alpha}$	−0.100	$\partial q_{C=O}/\partial \theta_{C_\alpha-C=O}$	−0.100
$\partial q_{OH}/\partial r_{HO}$	−0.110 (monomer)*	$\partial q_{C=O}/\partial \theta'_{C_\alpha-C-O}$	−0.030
	0.780 (dimer)	$\partial q_{C-O}/\partial \theta_{O-C=O}$	0.130*
$\partial q_{CC_\alpha}/\partial r_{CC_\alpha}$	−0.020	$\partial q_{C-O}/\partial \theta'_{C_\alpha-C=O}$	−0.065*
$\partial q_{O-C}/\partial r_{C-O}$	0.760 (monomer)	$\partial q_{C-O}/\partial \theta_{C_\alpha-C-O}$	−0.065*
	1.138 (dimer)	COH group	
$\partial q_{O=C}/\partial r_{C=O}$	0.680 (monomer)	$\partial q_{OH}/\partial \theta_{COH}$	0.050*
	0.550 (dimer)	$\partial q_{O-C}/\partial \theta_{COH}$	0.050*
$\partial q_{C_\alpha H}/\partial r'_{HC_\alpha}$	−0.035*		
$\partial q_{O\cdots H}/\partial r'_{C=O}$	0.240 (dimer)*		

a) e=electronic unit. b) The meanings of the symbols are the same as those reported previously (Refs. 4, 5). c) These values were chosen to satisfy the approximate redundancy conditions expressed by Eq. 4 (m=6); $2(\partial q_{C_\alpha H}/\partial \theta_{HC_\alpha H}) + \partial q_{C_\alpha H}/\partial \theta'_{HC_\alpha H} + \partial q_{C_\alpha H}/\partial \theta_{HC_\alpha C} + 2(\partial q_{C_\alpha H}/\partial \theta'_{HC_\alpha C}) = 0$ and $\partial q_{C_\alpha C}/\partial \theta_{HC_\alpha C} + \partial q_{C_\alpha C}/\partial \theta'_{HC_\alpha H} = 0$. d) These values are restricted by the redundancy conditions expressed by Eq. 4 (m=3); $\partial q_{C=O}/\partial \theta_{O-C=O} + \partial q_{C=O}/\partial \theta_{C_\alpha-C=O} + \partial q_{C=O}/\partial \theta'_{C_\alpha-C-O} = 0$ and $\partial q_{C-O}/\partial \theta_{O-C=O} + \partial q_{C-O}/\partial \theta'_{C_\alpha-C=O} + \partial q_{C-O}/\partial \theta_{C_\alpha-C-O} = 0$. The symbol * denotes the transferred value from formic acid or n-alkane.

angle between the dipole moment vector and the carbonyl bond of acetic acid monomer determined by the microwave spectra[19] is different from that of the trans conformer of formic acid monomer by 42°.[21] To make the effective atomic charges of acetic acid monomer consistent with the experimental dipole moment vector,[19] it was necessary to slightly adjust the β_{ki} of the C–H bond from 0.125 e of *n*-alkanes[5] to 0.150 e, and to introduce a relatively large homogeneous parameter γ_{li} for the C–C_α bond, 0.138 e. These bond charge parameters have been confirmed to explain the dipole moment vector of propionic acid[22] too, if supplemented with a small γ_{li} for the C_α–C_β bond. The bond charge parameters determined in this way are shown in Table 2, together with the bond charge fluxes. The charge fluxes for the three bending coordinates, θ_1—θ_3, around the carbonyl carbon atom and those for the six bending coordinates, θ_1—θ_6, around the methyl carbon atom should satisfy the redundancy condition:

$$\sum_{p=1}^{m} \frac{\partial q_{ij}}{\partial \theta_p} = 0 \ (m = 3 \text{ or } 6). \qquad (4)$$

This relation is not exact for the methyl group of acetic acid in which the H–C_α–H angles are about 2° smaller than the H–C_α–C angles. Since this difference was found to affect the simulated spectra only slightly in comparison with the calculation based on the exact redundancy condition (an intensification of the weak Raman band of acetic acid near 1410 cm^{-1} by less than 2%), we regarded Eq. 4 as an approximate redundancy condition for the methyl group. An appreciable reduction in the magnitude of the charge flux for the H–C_α bond from −0.216 of *n*-alkanes[5] to −0.100, was found necessary for fitting the calculated infrared absorption intensities of the H–C_α stretching modes to the intensity of the very weakly observed band. The angle bending fluxes for the acetyl group were newly estimated for acetic acid, while that concerning the C–O–H bending were transferred from formic acid. To reproduce the infrared absorption intensities of the C–O stretching mode coupled with the other modes in acetic acid dimer and its deuterated derivatives, we adopted a larger value of the C–O stretching charge flux than that used in formic acid dimer. The estimated infrared absorption intensity parameters are summarized in Table 2.

Raman Intensity Parameters. In analogy with the bond charges for the infrared absorption, our Raman intensity parameters consist of the equilibrium and the derived bond polarizabilities based on the bond polarizability model.[23-25] The equilibrium bond polarizability parameters concerning the carboxyl group were transferred from formic acid,[4] and those of the H–C_α and C–C_α bond from *n*-alkanes.[5a] The parameters for the C–C_α bond were then modified to explain the CNDO/2 and experimental polarizabilities.[26,27] In order to estimate the absolute values of the intensity parameters of acetic acid dimer, the intensity of the C–C_α stretching band of acetic acid was compared with the band at 802 cm^{-1} of cyclohexane, whose calculated absolute intensity was in good agreement with the observed value by Snyder, 24.0 $Å^4$ amu^{-1}.[28] The derived bond polarizabilities for the C–C_α stretching coordinate were taken from sodium acetate.[29] Although the intensity measurement for sodium acetate was made for crystalline powder samples, the transferred Raman intensity parameters successfully reproduced the observed ratio of the band intensities between acetic acid and cyclohexane in the liquid state. The observed and the simulated Raman spectra of a mixture of acetic acid and cyclohexane between 1000—700 cm^{-1} are shown in Fig. 1, where the half band widths in the simulation are set equal to the observed values. On transferring the derived polarizabilities used in *n*-alkanes[5] for the bending coordinates to the methyl group of acetic acid dimer, we obtained too large intensities of the CH_3 rocking modes. Thus, those derivatives with respect to

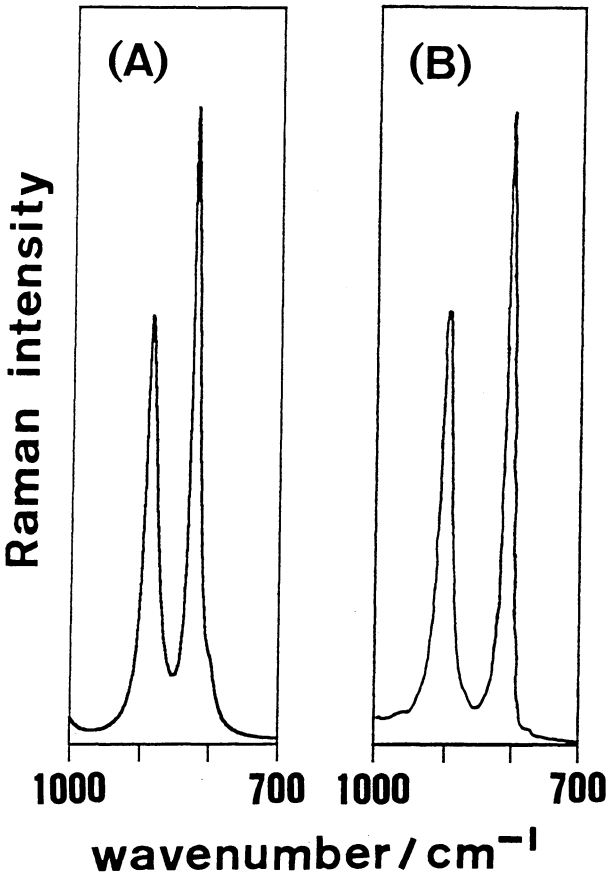

Fig. 1. Polarized Raman spectra of a liquid mixture of acetic acid and cyclohexane at room temperature: (A) Simulated, (B) Observed, recorded on a JEOL S-1 laser Raman spectrophotometer with a cooled HTV R649 photomultiplier, excited at 514.5 nm by a NEC GLG 3200 Ar^+ laser; slit width, 6 cm^{-1} at 1000 cm^{-1}. The scattering geometry is X(Z,Z)Y. The molar ratio of mixing, acetic acid dimer/cyclohexane, is 1.085.

the $HC_{\alpha}C$ bending coordinates adopted in *n*-alkanes were reduced by 60 to 70% for acetic acid. For the derived bond polarizabilities of the carboxyl group taken from formic acid,[4] no adjustment was found necessary except for those related to the bending coordinates around the carbonyl carbon atom. The derived parameter $\partial\gamma^{L}_{C=O}/\partial\theta_{O-C=O}$ could not be transferred from formic acid, since the transferred value was found to make the Raman band due to the O–C=O bending mode weaker than that due to the CO_2 rocking mode of acetic acid dimer. Two independent parameters $\partial\gamma^{L}_{C=O}/\partial\theta_{O-C=O}$ and $\partial\gamma^{L}_{C=O}/\partial\theta_{C\alpha-C=O}$ under the redundancy condition, Eq. 4, were so estimated as to give the best fit to the Raman intensities and depolarization ratios of the O–C=O bending and CO_2 rocking modes of acetic acid and its deuterated species. The adopted Raman intensity parameters are listed in Table 3.

Table 3. Bond Polarizabilities and Their Derivatives in Acetic Acid Monomer and Dimer

Equilibrium parameters[a]/Å[3b]			
$\gamma^{L}_{HC\alpha}$	0.290*	$\alpha^{E}_{HC\alpha}$	0.545*
$\gamma^{L}_{CC\alpha}$	1.230	$\alpha^{E}_{CC\alpha}$	0.265
$\gamma^{L}_{C=O}$	0.810*	$\alpha^{E}_{C=O}$	0.800*
γ^{L}_{C-O}	1.050*	α^{E}_{C-O}	0.540*
γ^{L}_{OH} (monomer)	0.300*	α^{E}_{OH}	0.500*
(dimer)	0.100*		
Derivatives for stretching coordinates[c]/Å[2b]			
$\partial\gamma^{L}_{HC\alpha}/\partial r_{HC\alpha}$	1.980*	$\partial\alpha^{E}_{HC\alpha}/\partial r_{HC\alpha}$	0.450*
$\partial\gamma^{L}_{CC\alpha}/\partial r_{CC\alpha}$	0.900	$\partial\alpha^{E}_{CC\alpha}/\partial r_{CC\alpha}$	1.000
$\partial\gamma^{L}_{C=O}/\partial r_{C=O}$	2.820*	$\partial\alpha^{E}_{C=O}/\partial r_{C=O}$	0.940*
$\partial\gamma^{L}_{C-O}/\partial r_{C-O}$	0.400*	$\partial\alpha^{E}_{C-O}/\partial r_{C-O}$	0.300*
Derivatives for bending coordinates/Å[3] rad[-1b]			
CH_3C group[d]			
$\partial\gamma^{L}_{HC\alpha}/\partial\theta_{HC\alpha H}$	−0.135	$\partial\gamma^{L}_{CC\alpha}/\partial\theta_{HC\alpha C}$	0.050
$\partial\gamma^{L}_{HC\alpha}/\partial\theta'_{HC\alpha H}$	0.200*	$\partial\gamma^{L}_{CC\alpha}/\partial\theta'_{HC\alpha H}$	−0.050
$\partial\gamma^{L}_{HC\alpha}/\partial\theta_{HC\alpha C}$	−0.030	$\partial\alpha^{E}_{CC\alpha}/\partial\theta_{HC\alpha C}$	0.070
$\partial\gamma^{L}_{HC\alpha}/\partial\theta'_{HC\alpha C}$	0.050	$\partial\alpha^{E}_{CC\alpha}/\partial\theta'_{HC\alpha H}$	−0.070
CO_2 group[e]			
$\partial\gamma^{L}_{C=O}/\partial\theta_{OC=O}$	−0.350	$\partial\gamma^{L}_{C=O}/\partial\theta_{C\alpha C=O}$	0.100
$\partial\gamma^{L}_{C=O}/\partial\theta'_{C\alpha C-O}$	0.250		
COH group			
$\partial\gamma^{L}_{HO}/\partial\theta_{COH}$	0.200*	$\partial\alpha^{E}_{HO}/\partial\theta_{COH}$	0.095*

a) The equilibrium parameters not followed by the parentheses are used commonly for the monomer and the dimer. b) 1 Å=10^{-10} m. 1 Å^3≃1.11265×10^{-40} C m^2 V^{-1}. c) Derivative parameters for the dimer. d) These values were chosen to satisfy the approximate redundancy conditions expressed by Eq. 4 (m=6); $2(\partial\gamma^{L}_{HC\alpha}/\partial\theta_{HC\alpha H})+\partial\gamma^{L}_{HC\alpha}/\partial\theta'_{HC\alpha H}+\partial\gamma^{L}_{HC\alpha}/\partial\theta_{HC\alpha C}+2(\partial\gamma^{L}_{HC\alpha}/\partial\theta'_{HC\alpha C})=0$, $\partial\gamma^{L}_{CC\alpha}/\partial\theta_{HC\alpha C}+\partial\gamma^{L}_{CC\alpha}/\partial\theta'_{HC\alpha H}=0$, and $\partial\alpha^{E}_{CC\alpha}/\partial\theta_{HC\alpha C}+\partial\alpha^{E}_{CC\alpha}/\partial\theta'_{HC\alpha H}=0$. e) These values are restricted by the redundancy condition expressed by Eq. 4 (m=3); $\partial\gamma^{L}_{C=O}/\partial\theta_{OC=O}+\partial\gamma^{L}_{C=O}/\partial\theta_{C\alpha C=O}+\partial\gamma^{L}_{C=O}/\partial\theta'_{C\alpha C-O}=0$. The symbol * denotes the transferred value from formic acid or *n*-alkane.

Half Band Width Parameters. For a variety of spectra, particularly for the vibrational spectra of polar compounds in the condensed phase, the band width is as important a quantity for characterizing a band as the frequency and the intensity. So far, we have assumed a homogeneous band width throughout a single scan of the vibrational spectrum of a pure compound, paying attention only to adjustment of the frequencies and the intensities. This simplification, initially adopted to avoid too much flexibility in estimating the intensity parameters, is valid when the spectral slit width of the instrument is broader than the band widths of all fundamentals inherent to the sample compound. In fact, our method has proved to be not so crude for *n*-alkanes and *n*-alkyl ethers[5] in the liquid phase, and for most of the Raman bands of formic acid in the gas phase.[4] For carboxylic acids in a condensed phase, however, we can no longer adhere to the approximation of homogeneous band width, since the extraordinarily broad width of the OH stretching band of dimeric carboxylic acids is well known. In the infrared absorption spectra, the OH out-of-plane deformation band is also very broad, while in the Raman spectra below 2000 cm^{-1}, the C=O stretching band and the CH_3 deformation bands of acetic acid are much broader than the others. It is thus desirable to distinguish the half band widths between different normal modes in a manner suitable for molecular mechanics, using any parametrization in which the local structures of molecules are properly reflected. Thus we introduce a half band width parameter, η_i, defined for each internal coordinate, say, R_i, in the spectral simulation hereafter. The half band width ω_a of the ath normal mode is calculated from the half band width parameter, η_i, and the element L_{ia} of the $\boldsymbol{L}$-matrix, as shown in Eq. 5:

$$\omega_a = \omega_0(\sum_i \eta_i L_{ia}^2 / \sum_i L_{ia}^2), \tag{5}$$

where ω_0 is the standard half band width and L_{ia} relates the ith internal coordinate with the normal coordinate as expressed by Eq. 6:

$$R_i = \sum_a L_{ia} Q_a \,. \tag{6}$$

The basic idea of this scheme is to assume that each internal coordinate, R_i, is associated with its own intrinsic band width characterized by η_i, in which all the broadening effects such as the anharmonicity and the intermolecular interaction are implicitly taken into account. The band width of a normal mode is given as an average of the intrinsic band widths weighted by the squared elements of the $\boldsymbol{L}$-matrix. The half band width parameters estimated empirically from the observed infrared absorption and Raman spectra of acetic acid at room temperature are shown in Table 4. These parameters have been chosen as a minimal essential set necessary for reproducing the observed variation in the

Table 4. Half Band Width Parameters[a)]

Internal coordinate		η_i[b)]
OH	stretching (dimer)	70.0
COH	bending	6.0
OH···O	out-of-plane bending (dimer)	8.0
$HC_\alpha H$	bending	2.0
$HC_\alpha C$	bending	2.0

a) The parameters not followed by the parentheses are used commonly for the monomer and the dimer. b) The half band width parameter for the internal coordinates not listed in Table 4 is 1.0.

half band widths. A single set of half band width parameters was used commonly for the infrared absorption and Raman spectra of acetic acid, and the difference in the adopted optical slit width was taken into account by attributing different values of the standard half band width ω_0 in Eq. 5 to these two spectra. In the spectral simulation, each band contour is assumed to be reprensented by a Lorentzian function.[4,5)]

Results and Discussion

The experimental and the calculated values of the structure parameters, the heats of formation, the entropies, the molecular dipole moment and the polarizability of acetic acid monomer and/or dimer are listed in Tables 5 and 6. The calculated geometries of the monomer and the dimer are in good agreement with the experiment. The calculalted entropy of the monomer is close to the experimental value,[30)] while that of the dimer is not so good probably because of the crudeness of the harmonic approximation for the low-frequency intermonomer vibrational modes. The molecular dipole moment and the polarizability tensor were calculated to agree well with the experimental and the CNDO/2 values,[21,26,27)] respectively. The calculated barrier about the C–O bond, 60.4 kJ mol^{-1}, is comparable with the ab initio values, 55.1 kJ mol^{-1} [32)] and 61.9 kJ mol^{-1}.[33)]

The experimental and the calculated values of the vibrational frequencies and the infrared absorption intensities of acetic acid dimer and its deuterated deriv-

Table 5. Experimental and Calculated Equilibrium Geometries, Heats of Formation, Entropies for Acetic Acid Monomer and Dimer

Geometry[a)]	Monomer		Dimer	
	Exptl[b)]	Calcd	Exptl[c)]	Calcd
r(O–H)/Å	0.970	0.998	1.03	1.052
r(C–O)/Å	1.357	1.355	1.334	1.337
r(C=O)/Å	1.209	1.210	1.231	1.228
r(C–C_α)/Å	1.494	1.495	1.506	1.500
r(H–C_α)/Å	1.090	1.087[d)]	1.102	1.089[d)]
r(O···O)[e)]/Å	—	—	2.684	2.706
r(O···O)[f)]/Å	—	—	2.259	2.257
∠(O–H···O)/°	—	—	—	173.2
∠(C–O–H)/°	105.9	107.3	110.0	109.9
∠(O–C=O)/°	122.8[c)]	121.5	123.4	123.2
∠(C_α–C–O)/°	112.0	112.2	113.0	113.7
∠(C_α–C=O)/°	126.2	126.3	123.6	123.1
∠(H–C_α–H)/°	109.5	108.4[d)]	—	108.5[d)]
∠(H–C_α–C)/°	—	110.6[d)]	—	110.5[d)]
	Heat of formation and entropy (at 298.15 K)			
	Exptl	Calcd	Exptl	Calcd
ΔH_f^0/kJ mol^{-1}	−432.8[g)]	−432.3	−927.5[h)]	−927.7
S/J mol^{-1} deg^{-1}	283[i)]	286	420[h)]	412
	Dimerization energy (at 298.15 K)			
	Exptl	Calcd		
ΔH_D/kJ mol^{-1}	−61.9± 4.2[j)]	−63.1		
ΔS_D/J mol^{-1} deg^{-1}	−145.6± 8.4[j)] −175 ±11[k)]	−160		

a) 1 Å=10^{-10} m. b) van Eijck et al., Ref. 9. c) Derissen, Ref. 10. d) Averaged value. e) Hydrogen-bonded distance in the dimer. f) Intramolecular distance between the oxygen of the hydroxyl group and that of the carbonyl group. g) Pedley et al., Ref. 6. h) Estimated from the enthalpy ΔH_D and the entropy ΔS_D of dimerization (Ref. 7). i) Stull et al., Ref. 30. j) Clague and Bernstein, Ref. 7. k) Lumbroso-Bader et al., Ref. 31.

Table 6. Molecular Dipole Moment and Polarizability of Acetic Acid Monomer

	Molecular dipole moment	
	Exptl	Calcd
μ/Debye	1.70[a]	1.64
Direction/°	0[a]	3[a]
	Molecular polarizability/10^{-40} C m^2 V^{-1}	
	CNDO/2[b] (Exptl[c])	Calcd
α_X	6.46[d]	6.47[e]
α_Y	6.11	6.16
α_Z	4.93[d]	4.59
α (average)	5.83 (6.35)	5.74

a) Kim et al., Ref. 21. The direction of the dipole moment is defined as the angle formed between the C=O bond and the moment (Stiefvater, Ref. 22). b) Rhee et al., Ref. 26. c) The value cited by Lippincott et al., Ref. 27. d) X-axis is along the C–C$_\alpha$ bond and Z-axis is perpendicular to the plane containing the carboxyl group. e) The angle formed by the X-axis and the C–C$_\alpha$ bond is 10 deg.

atives are shown in Table 7. The observed intensities[35] of the infrared absorption bands due to the OH out-of-plane deformation modes of acetic acid dimer and the corresponding bands of deuterated acetic acids, which are useful in estimating the charges of the hydroxyl group,[4] roughly coincide with the calculated intensities. The OH stretching charge flux of acetic acid dimer, being slightly modified from that adopted in formic acid,[4] reproduces well the experimental infrared absorption intensity of the OH stretching mode.[35] The mutually exclusive infrared absorption and Raman frequencies were successfully simulated with reasonable accuracy, except for the out-of-plane CD_3 rocking frequencies of acetic-d_3 acid and its O-deuterated compound. Probably, simultaneous fitting of the in-plane and the out-of-plane CH_3 and CD_3 rocking frequencies requires independent adjustment of the force constants for the H–C$_\alpha$–C angles in and out of the C$_\alpha$–C=O plane. The overall order of the calculated infrared absorption intensities follows well the observed trend.[35] In respect of several sets of hardly separable bands for which the total intensities had been measured by Marechal,[35] our calculated intensity sums closely reproduced the experimental results. Furthermore, comparison between the gaseous spectra of isotopic acetic acids reported by Haurie and Novak[12] suggests that the calculated intensities of the individual normal modes contributing to the above sums are mostly correct. The isotope effect on the O-deuteration of acetic acid is reflected in the marked intensity decrease of $\delta_{as}CH_3$ on the decoupling between $\delta_{as}CH_3$ and δOD, while the effect of perdeuteration is reflected in the large intensity increase of νC–O on the decoupling of $\delta_{as}CD_3$ and δOD from νC–O. The C-deuteration of acetic acid causes the intensification of δOH and νC–O and the weakening of $\delta_{as}CD_3$ and δ_sCD_3. Thus, calculation of infrared absorption intensities is very helpful for understanding the intramolecular vibrational perturbation on the isotopic substitution.

Previous workers[36,38] assigned the B_u hydrogen-bond stretching mode of the gaseous acetic acid dimer to the infrared doublet at 168/188 cm^{-1} involved in a Fermi resonance. Recently, Zelsmann et al.[17] have estimated the band center of the mode to be at 171 cm^{-1} by means of the "peeled-off" spectra, in which the effect of the Fermi resonance has been eliminated. The use of the Morse potential parameters for the hydrogen bond transferred from formic acid dimer[4] has proved to be successful in reproducing the hydrogen-bonding stretching frequencies of acetic acid dimer and its deuterated species, particulary those of the B_u modes, observed in the gas phase.[17] In the Raman spectra of liquid phase, Nielsen and Lund[18] assigned a band at 55 cm^{-1} to the A_g O–H··· O deformation mode. Bertie and Mechaelian,[39] however, concluded that the band at 55 cm^{-1} has no analogue in the spectra of the gas phase and it is reassigned to an intermolecular pseudolattice mode of the liquid. According to the Fermi resonance analysis by Zelsmann et al.,[17] the A_g O–H···O deformation frequency is located at 120 cm^{-1}, which is comparable with our calculated value, 146 cm^{-1}. The observed frequency of the B_g O–H···O out-of-plane mode, 106 cm^{-1} [40] in the gas phase and 115 cm^{-1} [18] in the liquid phase, agrees with our value.

The calculated frequencies and infrared absorption intensities of acetic acid mononer and its deuterated compounds are compared with those observed in Table 8. There has been much controversy as to the assignments of normal modes contributed by the C–O stretching and the C–O–H deformation vibrations of the monomer.[13-16] Unusual participation of the anharmonicity in these modes has been pointed out by Bernay et al.[16] on their interpretation of the matrix isolation spectra. Except for the cases related to these modes, our calculation, which is based mostly on the transferred potential and intensity parameters, reproduces the expeprimental results[15,16,35] fairly well.

The half band widths of acetic acid dimer calculated by using the half band width parameters η_i defined above are compared with those observed in the solution and the liquid phase in Table 9. The large value of η(OH) reproduces the observed broad band width of the OH stretching mode in the infrared absorption spectra of acetic acid in the carbon tetrachloride solution. Numerous theoretical and experimental works[1-3,35,42-45] have been carried out on the peculiar feature of the infrared absorption band due to the OH stretching mode. According to Maréchal,[35,42-44] the complex band in the gas phase arises mainly from the modulation of the OH stretching made by intermonomer modes and the Fermi resonance with overtone and combination levels. The large half band width parameter introduced for the OH stretching internal coordinate would explain the band

Table 7. Experimental and Calculated Vibrational Frequencies and Infrared Absorption Intensities for Acetic Acid Dimer and Its Deuterated Species

	Freq./cm^{-1}					IR int./km mol^{-1}			
	Exptl[a]			Calcd		Exptl		Calcd	Assignments[a]
	Gas	Liq	Liq			Gas/Liq[a]	Gas[b]		
			$(CH_3COOH)_2$						
No.	B_u		A_g	B_u	A_g				
1	3027	3028	**	3075	3074	s/s	2431	2443.1	νOH
2	**	**	3032	2992	2992			3.7	$\nu_{as}CH_3$
3	**	**	2949	2937	2937			18.9	ν_sCH_3
4	1730	1715	1675	1726	1670	vs/vs	764	780.9	νC=O
5	1422	1413	1436	1416	1445	m/m#	229[c]	120.6	δOH§
6	1422	1413	1436	1407	1410	m/m#	No. 5[c]	55.0	$\delta_{as}CH_3$
7	1365	1359	1370	1367	1369	sh/w		68.3	δ_sCH_3
8	1292	1295	1283	1280	1278	s/s	310	312.6	νC–O§
9	1005	1013	1018	1015	1013	m/w	No. 18[d]	2.5	ρ_sCH_3
10	890	886	886	887	886	sh/vw	No. 18[d]	13.2	νC–C$_\alpha$
11	621	624	624	641	634	m/m	37.4	41.1	δO–C=O
12	475	480	448	479	444	m/m		17.9	ρCO_2
13	171[e]	184[f]	165[g]	162	202			7.6	νO···O[h]
14	—	—	120[e]	—	146	—	—	—	δO–H···O ipb[h]
	A_u		B_g	A_u	B_g				
15	**	**	3000	2997	2997			1.0	$\nu_{as}CH_3$
16	1422	1413	1436	1412	1412	m/m#	No. 5[c]	0.1	$\delta_{as}CH_3$
17	1060	1050	n.o.	1039	1039	w/w	No. 18[d]	24.7	$\rho_{as}CH_3$
18	940	934	n.o.	938	913	m/m	192[d]	139.8	γOH
19	**	**	**	560	565			5.3	πCO_2
20	56[e]		115[g]	63	120			8.9	δO–H···O opb[h]
21	n.o.[e]		n.o.[g]	95	89			0.4	τC–C$_\alpha$
22	49[e]		—	70	—			0.0	Twist CO_2[h]
			$(CH_3COOD)_2$						
No.	B_u		A_g	B_u	A_g				
1	3050	**	3028	2992	2992	sh/		3.5	$\nu_{as}CH_3$
2	2950	**	2946	2940	2940	w/		12.8	ν_sCH_3
3	2270	2268	n.o.	2238	2245	s/s	1047	1384.4	νOD
4	1732	1715	1651	1718	1658	vs/vs	554	739.4	νC=O
5	1430	1418	1434	1411	1411	sh/sh#		10.3	$\delta_{as}CH_3$
6	1395	1388	1374	1380	1381	s/s	No. 7[i]	245.4	δ_sCH_3§
7	1325	1322	1324	1316	1316	s/s	463[i]	209.2	δC–O§
8	1062	1055	1092	1065	1083	m/m##	36.2	65.5	δOD
9	1002	1000	1012	1009	1010	m/m	No. 17[j]	0.4	ρ_sCH_3
10	850	835	858	855	856	w/w		14.0	νC–C$_\alpha$
11	602	605	595	619	608	m/m	48.3	35.6	δO–C=O
12	468	472	443	469	436	m/m		19.4	ρCO_2
13	167[e]		165[g]	160	200			7.3	νO···O[h]
14	—	—		—	144	—	—	—	δO–D···O ipb[h]

a) Haurie and Novak, Ref. 12. b) The observed IR intensity A_i(km mol^{-1}) of the ith normal mode is estimated by the following equation (Ref. 34): A_i=0.1·Γ_i (m^2 mol^{-1})·$\bar{\nu}_i$ (cm^{-1}), where Γ_i and $\bar{\nu}_i$ are the intensity and the band center of the ith mode, respectively, observed by Maréchal (Ref. 35). For the sum of the Γs of the hardly separable bands, the band centers of the related modes were averaged (see footnote g in Table 4 of Ref. 4a). For each isotope, the intensity of the mode labeled with No. I has been added to the intensity of the mode No. I; see Ref. 35. Here the dimer is regarded as a molecular unit. c) The intensity sum of No. 5, 6, 16 is given for No. 5. d) The intensity sum of No. 9, 10, 17, 18 is given for No. 18. e) Zelsmann et al., Ref. 17. f) Jakobsen et al., Ref. 36. g) Nielsen and Lund, Ref. 18. h) Yokoyama et al., Ref. 4. i) The intensity sum of No. 6, 7 is given for No. 7. j) The intensity sum of No. 9, 17 is given for No. 17. k) The intensity sum of No. 5, 6 is given for No. 6. l) Fukushima and Zwolinski, Ref. 37. m) The intensity sum of No. 9, 10, 17, 18 is given for No. 18. n) The intensity sum of No. 6, 7 is given for No. 6. Abbreviation; **: masked, n.o.: not observed, #, ##: overlapping band, §: vibrational coupling, vs: very strong, s: strong, m: medium, w: weak, vw: very weak, sh: shoulder ν: stretching, δ: bending, ρ: rocking, γ: out-of-plane bending, τ: torsion, π: CO_2 out-of-plane bending, subscript as: antisymmetric, subscript s: symmetric.

Table 7. (Continued)

	Freq./cm^{-1}					IR int./km mol^{-1}			
	Exptl[a]			Calcd		Exptl		Calcd	Assignments[a]
	Gas	Liq	Liq			Gas/Liq[a]	Gas[b]		
			$(CH_3COOD)_2$						
No.	A_u		B_g	A_u	B_g				
15	2985	**	2995	2997	2997	w/		1.0	$\nu_{as}CH_3$
16	1430	1418	1434	1412	1412	sh/sh#		0.2	$\delta_{as}CH_3$
17	1062	1055	1057	1039	1039	m/m##	44.2[j]	24.2	$\rho_{as}CH_3$
18	702	697	n.o.	687	658	m/m	70.8	86.0	γOD
19	**	**	**	551	565			0.5	πCO_2
20	56[e]		112[g]	63	120			8.7	δO–D···O opb[h]
21	n.o.[e]		n.o.[g]	95	88			0.5	τC–C$_\alpha$
22	48[e]		—	70	—			0.0	Twist CO_2[h]
			$(CD_3COOH)_2$						
No.	B_u		A_g	B_u	A_g				
1	3040	3028	n.o.	3072	3070	s/s	2338	2455.5	νOH
2	2280	2250	2278	2191	2191	vw/vw		4.4	$\nu_{as}CD_3$
3	2115	2110	2118	2116	2116	vw/vw		0.3	ν_sCD_3
4	1732	1710	1657	1719	1662	vs/vs	799	787.0	νC=O
5	1408	1408	1430	1408	1442	m/m	No. 6[k]	130.9	δOH§
6	1299	1297	1294	1293	1293	s/s	543[k]	389.5	νC–O§+νC–C$_\alpha$[l]
7	1078	1080	1090	1098	1097	w/w	17.3	9.3	δ_sCD_3
8	1052	1030	1044	1024	1024	w/w#		0.1	$\delta_{as}CD_3$
9	828	823	828	820	814	m/m	No. 18[m]	4.4	ρ_sCD_3
10	**	**	841	804	801		No. 18[m]	4.2	νC–C$_\alpha$+ρ_sCD_3
11	595	598	601	610	610	m/m	35.8	44.5	δO–C=O
12	430	434	399	447	410	m/m		12.0	ρCO_2
13	158[e]			150	196			6.7	νO···O[h]
14	—	—		—	142	—	—	—	δO–H···O ipb[h]
	A_u		B_g	A_u	B_g				
15	2235	2250	2245	2193	2193	sh/vw		0.5	$\nu_{as}CD_3$
16	1052	1030	1044	1019	1019	w/w#		0.0	$\delta_{as}CD_3$
17	942	924	931	853	853	m/m##	No. 18[m]	12.5	$\rho_{as}CD_3$
18	942	924	n.o.	938	914	m/m##	145[m]	146.7	γOH
19	**	510	517	517	523	/vw		4.0	πCO_2
20	53[e]			58	114			5.3	δO–H···O opb[h]
21	n.o.[e]			85	65			0.8	τC–C$_\alpha$
22	46[e]		—	55	—			1.7	Twist CO_2[h]
			$(CD_3COOD)_2$						
No.	B_u		A_g	B_u	A_g				
1	2283	2278	**	2240	2246	s/s	1001	1381.3	νOD
2	**	**	2276	2191	2191			5.3	$\nu_{as}CD_3$
3	**	**	2116	2115	2116			8.3	ν_sCD_3
4	1725	1708	1651	1711	1650	vs/vs	553	745.5	νC=O
5	1357	1355	1340	1339	1341	s/s	353	435.8	νC–O+νC–C$_\alpha$[l]
6	1085	1087	1090	1060	1077	m/m	41.6[n]	40.1	δOD
7	1052	1047	1090	1098	1099	m/m	No. 6[n]	16.7	δ_sCD_3
8	1030	1033	1042	1018	1020	sh/sh#		6.7	$\delta_{as}CD_3$
9	828	831	832	815	811	m/m		6.4	ρ_sCD_3
10	803	800	799	775	773	m/vw	33.6	4.6	νC–C$_\alpha$
11	581	581	577	596	590	m/m	70.0	41.0	δO–C=O
12	425	425	399	438	402	m/m		13.2	ρCO_2
13	156[e]		160[g]	148	194			6.4	νO···O[h]
14	—	—		—	141	—	—	—	δO–D···O ipb[h]

Table 7. (Continued)

No.	Freq./cm^{-1} Exptl[a] Gas	Exptl Liq	Exptl Liq	Calcd		IR int./km mol^{-1} Exptl Gas/Liq[a]	Exptl Gas[b]	Calcd	Assignments[a]
			$(CD_3COOD)_2$						
	A_u		B_g	A_u	B_g				
15	**	**	2240	2193	2193			0.5	$\nu_{as}CD_3$
16	1030	1033	1042	1019	1019	sh/sh#		0.4	$\delta_{as}CD_3$
17	930	926	926	854	854	m/m	16.7	23.8	$\rho_{as}CD_3$
18	694	692	n.o.	684	658	m/m	55.2	79.1	γOD
19	**	505	510	510	523	/vw		0.9	πCO_2
20	52[e]		108[g]	58	113			5.0	δO–D···O opb[h]
21	n.o.[e]		n.o.[g]	85	65			0.9	$\tau C–C_\alpha$
22	45[e]		—	55	—			1.8	Twist CO_2[h]

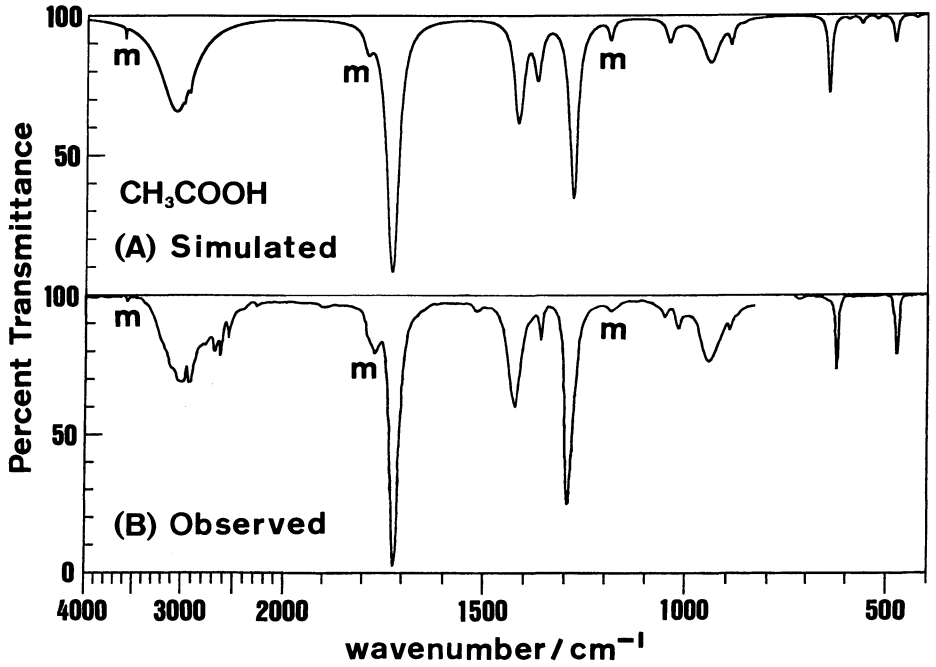

Fig. 2. Infrared spectra of acetic acid in CCl_4 solution at room temperature: (A) Simulated (ω_0=10 cm^{-1}) and (B) Observed. The monomer bands are indicated as **m**. The spectra was measured with a JASCO IRA-2 IR spectrometer: slit width 1.5 cm^{-1} at 1000 cm^{-1}; path length 0.1 mm. The concentration of acetic acid was 0.161 mol dm^{-3}.

width of the complex band empirically, though the assumption of a simple Lorentzian envelope should be modified for more detailed comparison between the observed and the simulated band shapes. The other half band width parameters in Table 4 roughly reproduce the observed half band widths at room temperature as shown in Table 9.

The simulated and the observed infrared absorption spectra of acetic acid in the carbon tetrachloride solution are shown in Fig. 2. The band intensities observed in the condensed phase should be corrected for the effect of the internal electric field, for which a few equations have been proposed. According to the Polo–Wilson equation[46] widely used for the pure liquids and solutions, the infrared absorption intensities in a dilute solution are greater than those in the gas phase. As the refractive index n_D of carbon tetrachloride is approximately 1.46, the calculated intensities should be multiplied by a correction factor of 1.30. On the contrary, according to Akiyama's revised equation,[47,48] the corrected intensities for n_D=1.46 are 94.3% of those in the gas phase. In this work, the Polo–Wilson equation was found to give closer fit to the experimental than the Akiyama equation for acetic acid in the carbon tetrachloride solution, as far as

Table 8. Experimental and Calculated Vibrational Frequencies and Infrared Absorption Intensities for Acetic Acid Monomer and Its Deuterated Species

	Freq./cm^{-1}			IR int./km mol^{-1}			Assignments[b]
	Exptl[a]			Exptl			
	Ref.15	Ref. 16	Calcd	Ref. 15	Ref. 35	Calcd	
CH_3COOH							
A′ No.							
1	3583	3566	3602	m	57.3	72.7	νOH
2	3051		3001	vw		1.6	$\nu_{as}CH_3$
3	2944		2950	vw		3.9	ν_sCH_3
4	1788	1779	1787	vs	304	304.3	νC=O
5	1430	1434	1413	sh#		0.6	$\delta_{as}CH_3$
6	1382	1380	1373	m	83.7	36.9	δ_sCH_3§
7	1264	1181	1241	m	76.8	78.1	δOH§
8	1182	1259	1187	s	177	176.7	νC–O§
9	989	987	1003	m	No. 15[d]	6.1	ρ_sCH_3
10	847		858	w		22.7	νC–C$_\alpha$
11	642	581	591			18.1	δO–C=O
12	581	428	426			22.4	ρCO_2
A″							
13	2996		3011	vw		0.5	$\nu_{as}CH_3$
14	1430	1439	1413	sh#		0.1	$\delta_{as}CH_3$
15	1048	1044	1044	w	61.9[d]	13.3	$\rho_{as}CH_3$
16	642[e]	639[e]	641	ms		128.3	γOH
17	534[e]	535[e]	523	m		20.1	γCCO
18	93[f]		95			0.1	τCH_3
CH_3COOD							
A′ No.							
1	3039		3001	vw		1.5	$\nu_{as}CH_3$
2	2952		2950	vw		3.6	ν_sCH_3
3	2642	2631	2620	m	34.4	42.9	νOD
4	1775	1770	1782	vs	276	284.0	δC=O
5	1440	1429	1413	sh#		0.7	$\delta_{as}CH_3$
6	1383	1377	1372	s	69.8	34.3	δ_sCH_3§
7	1270	1271	1187	s	152	189.8	νC–O§
8	990	956	1017	sh	No. 9[g]	33.8	ρ_sCH_3
9	955	1267	960	s	100[g]	21.5	δOD
10	840	835	820	w		19.2	νC–C$_\alpha$
11	603	545	574		12.1	15.1	δO–C=O
12	543	418	419			23.2	ρCO_2
A″							
13	2997		3011	vw		0.5	$\nu_{as}CH_3$
14	1440	1435	1413	sh#		0.1	$\delta_{as}CH_3$
15	1052	1051	1044	w	No. 9[g]	13.0	$\rho_{as}CH_3$
16	603	604	581	m		33.2	γCCO
17	415	422	425	m		51.9	γOD
18	93[f]		95			0.1	τCH_3

a) Observed frequencies of the monomer in vapor phase (Ref. 15) and those in an argon matrix (Ref. 16). b) Haurie and Novak, Ref. 15. c) The observed IR intensities were estimated on the basis of Maréchal's experimental data (Ref. 35). See footnote b in Table 7. d) The intensity sum of No. 9, 15 is given for No. 15. e) Assignments interchanged. f) Calculated value by Haurie and Novak, Ref. 15. g) The intensity sum of No. 8, 9, 15 is given for No. 9. h) The intensity sum of No. 5, 6, 7 is given for No. 6. i) The bands at 1225 cm^{-1} and 1170 cm^{-1} were assigned to the νC–O mode (Ref. 35). j) Nakamoto and Kishida, Ref. 41. k) The intensity sum of No. 9, 10, 15 is given for No. 15. l) The intensity sum of No. 11, 16 is given for No. 16. Abbreviation: **: masked, #: overlapping band, §: vibrational coupling, ν: stretching, δ: bending, ρ: rocking, γ: out-of-plane bending, τ: torsion, subscript as: antisymmetric, subscript s: symmetric.

Table 8. (Continued)

	Freq./cm^{-1}			IR int./km mol^{-1}			Assignments[b]
	Exptl[a]			Exptl			
	Ref.15	Ref. 16	Calcd	Ref. 15	Ref. 35[c]	Calcd	
CD_3COOH							
A′ No.							
1	3582	3563	3602	m	57.2	72.8	νOH
2	2285		2198	vw		1.4	$\nu_{as}CD_3$
3	2118		2126	vw		1.2	ν_sCD_3
4	1783	1774	1780	vs	303	303.1	νC=O
5	1338	1208	1241	m	No. 6[h]	115.9	δOH§
6	1167[i]	1332[i]	1208	s	355[h]	139.2	νC–O§+νC–C$_\alpha$[j]
7	1078	1157	1081	m	No. 6[h]	38.2	δ_sCD_3
8	1055	1034	1023	m		0.5	$\delta_{as}CD_3$
9	819	817	816	w	No. 15[k]	6.8	ρ_sCD_3
10	**		769		No. 15[k]	7.6	νC–C$_\alpha$
11	615	563	563		No. 16[l]	22.6	δO–C=O
12	478	408	396			16.6	ρCO_2
A″							
13	2230		2203	vw		0.3	$\nu_{as}CD_3$
14	1038	1070	1020	sh		0.1	$\delta_{as}CD_3$
15	918	919	857	w	34.7[k]	15.4	$\rho_{as}CD_3$
16	560	610[e]	631		113[l]	132.1	γOH
17	560	479[e]	489			10.2	γCCO
18	66[f]		69			0.2	τCD_3
CD_3COOD							
A′ No.							
1	2642	2633	2602	m	37.0	42.7	νOD
2	2275		2198	vw		1.3	$\nu_{as}CD_3$
3	2116		2126			1.1	ν_sCD_3
4	1775	1766	1775	vs	285	282.7	νC=O
5	1300	1296	1209	s	234	189.0	νC–O+νC–C$_\alpha$[j]
6	1080	1001	1084	m	34.5	52.9	δ_sCD_3
7	1056	1035	1029	m#		4.8	$\delta_{as}CD_3$
8	1004	1268	951	m	55.3	24.4	δOD
9	813	818	816	w		6.9	ρ_sCD_3
10	**		738			8.4	νC–C$_\alpha$
11	540	531	551	m		20.2	δO–C=O
12	**		389			17.3	ρCO_2
A″							
13	2240		2203	vw		0.3	$\nu_{as}CD_3$
14	1056	1073	1020	m#		0.2	$\delta_{as}CD_3$
15	917	919	857	w		12.8	$\rho_{as}CD_3$
16	528	531	548	m		38.9	γCCO
17	408	409	414	w		42.3	γOD
18	66[f]		69			0.2	τCD_3

no changes of the charge distribution on the phase change were assumed. The simulation was performed by superimposing the spectra of the monomer and the dimer with the monomer/dimer ratio calculated from the experimental free energy of dimerization,[7] 1/23 in moles of monomeric unit. As a result, the overall tendencies in the frequencies, the intensities and the band widths are successfully reproduced. Because of the crudeness of the calculated entropy of dimerization mentioned above, the use of the calculated free energy gives the monomer/dimer ratio, 1/12, which makes the monomer bands too strong as compared with the observed spectra. To check the transferability of the half band width parameters, we also simulated the infrared absorption spectrum of formic acid dissolved in carbon tetrachloride, assuming no other solvent–solute interaction

Table 9. Half Band Widths of Acetic Acid

		IR active modes (ω_0=10 cm^{-1})			Raman active modes (ω_0=12 cm^{-1})		
		Freq.	Half band width		Freq.	Half band width	
		cm^{-1}	cm^{-1}		cm^{-1}	cm^{-1}	
		Calcd	Calcd	Exptl	Calcd	Calcd	Exptl
No.		B_u			A_g		
1	νOH	3075	371.2	386	3074	—	—
2	νC=O	1726	20.2	15[a)]	1670	32.9	44
3	δOH	1416	22.0	29#	1445	26.1	54#
4	$\delta_{as}CH_3$	1407	21.4	#	1410	24.1	#
5	$\delta_s CH_3$	1367	20.8	10	1369	24.3	20[b)]
6	νC–O	1280	19.2	17	1278	22.5	24[b)]
7	$\rho_s CH_3$	1015	19.7	14[c)]	1013	23.5	22[b)]
8	νC–C$_\alpha$	887	11.9	10[c)]	886	16.2	14
9	δO–C=O	641	10.5	10	634	14.3	13
10	ρCO_2	479	11.2	11	444	14.1	14
		A_u			B_g		
11	$\delta_{as}CH_3$	1412	20.0	#	1412	24.0	#
12	$\rho_{as}CH_3$	1039	18.9	15[c)]	1039	23.0	
13	γOH	938	49.8	51	913	61.9	

a) Estimated from the observed spectra in which the concentration of acetic acid was 0.0924 mol dm^{-3}. b) Estimated from the observed spectra measured with approximately ten times as high sensitivity as that for Fig. 4. c) Estimated from the observed spectra in which the concentration of acetic acid was 0.411 mol dm^{-3}. Abreviation: ν: stretching, δ: bending, ρ: rocking, γ: out-of-planing, τ: torsion, subscript as: antisymmetric, subscript s: symmetric, #: overlapping band.

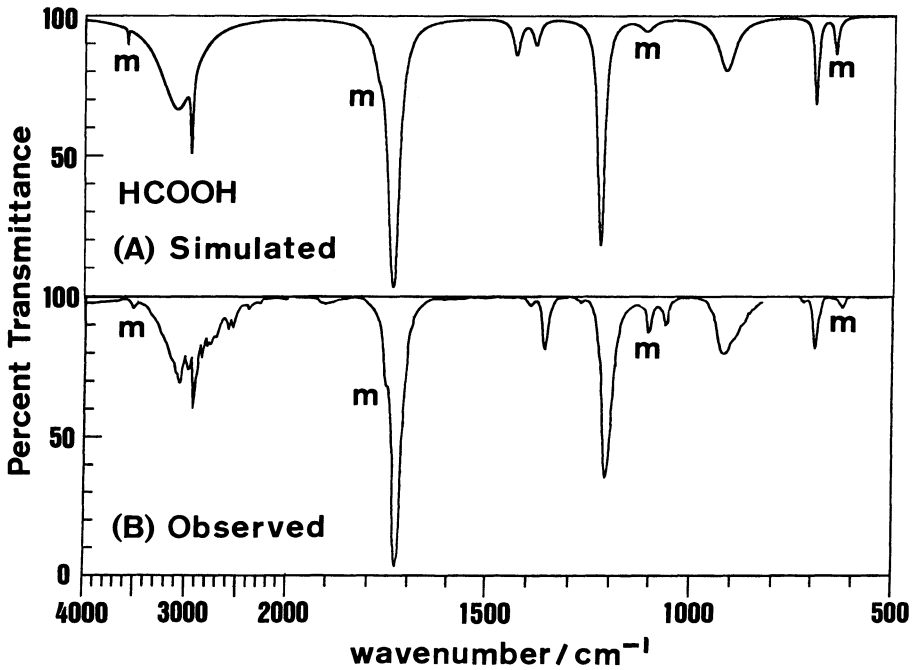

Fig. 3. Infrared spectra of formic acid in CCl_4 solution at room temperature: (A) Simulated (ω_0=10 cm^{-1}) and (B) Observed. The monomer bands are indicated as **m**. The concentration of formic acid was 0.197 mol dm^{-3}. For the other experimental conditions, see caption of Fig. 2.

than that implicitly incorporated in η_i's. The potential and the intensity parameters for the gaseous formic acid monomer and dimer[4] were used together with the η_i's for acetic acid except for $\eta(HC_\alpha C)$ and $\eta(HC_\alpha H)$, and the intensity at each wavenumber was multiplied by the internal field factor, 1.30, as in the case of acetic acid. Obviously, the dimer is predominant in the observed spectrum of formic acid, whereas the monomer/dimer ratio predicted from our potential model, in which the Morse parameters D and α for the OH bond are fitted to the enthalpy of dimerization in the gas phase estimated by Henderson,[8] is 1/0.6. Accordingly, we simulated the spectrum by using the monomer/dimer ratio of formic acid, 1/18, calculated from the free energy dimerization reported by Clague and Bernstein.[7] The overall patterns and the peak intensities of the simulated spectrum follow well those of the experimental spectrum as shown in Fig. 3, giving supports to the η_i's for the carboxyl group and also to the use of the Polo–Wilson equation[46] for carboxylic acid. To settle the problem of the internal field correction, however, more data on the spectral change on the phase change of many other compounds should be accumulated, since the Akiyama equation has proved to work well on simulating the infrared spectrum of *n*-alkyl ethers dissolved in carbon tetrachloride by using the intensity parameters estimated for the gas phase.[5]

The simulated and observed polarized Raman spectra of acetic acid and its perdeuterated species in the liquid phase are shown in Fig. 4 and 5. Since the neutron diffraction data were reported to be elucidated well by the cyclic dimer structure,[49] we ignored the other components in the Raman spectral simulation of liquid acetic acid. In this work, the sensitivity correction was made on the simulated spectra, since the correction on the observed spectra was complicated by the skewness of a

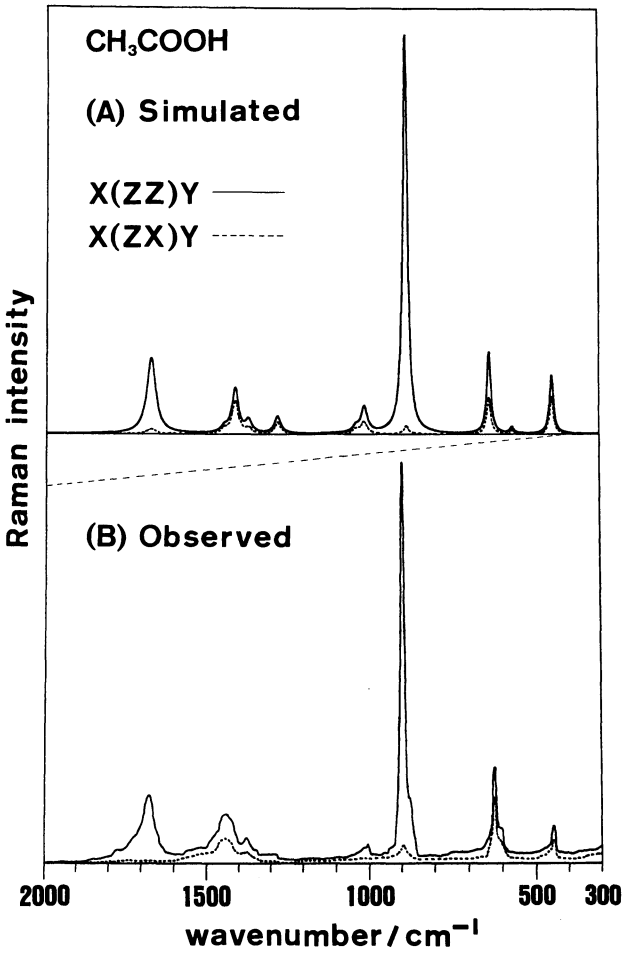

Fig. 4. Polarized Raman spectra of liquid acetic acid: (A) Simulated (ω_0=12 cm^{-1}) and (B) Observed. The experimental conditions, see caption of Fig. 1. The dashed line in the observed spectra indicates the frequency dependence of sensitivity of the detector (HTV R649 photomultiplier). The full scale of the simulated spectra was adjusted according to this sensitivity. The scattering geometry is X(Z,Z)Y (solid line) and X(Z,X)Y (dotted line).

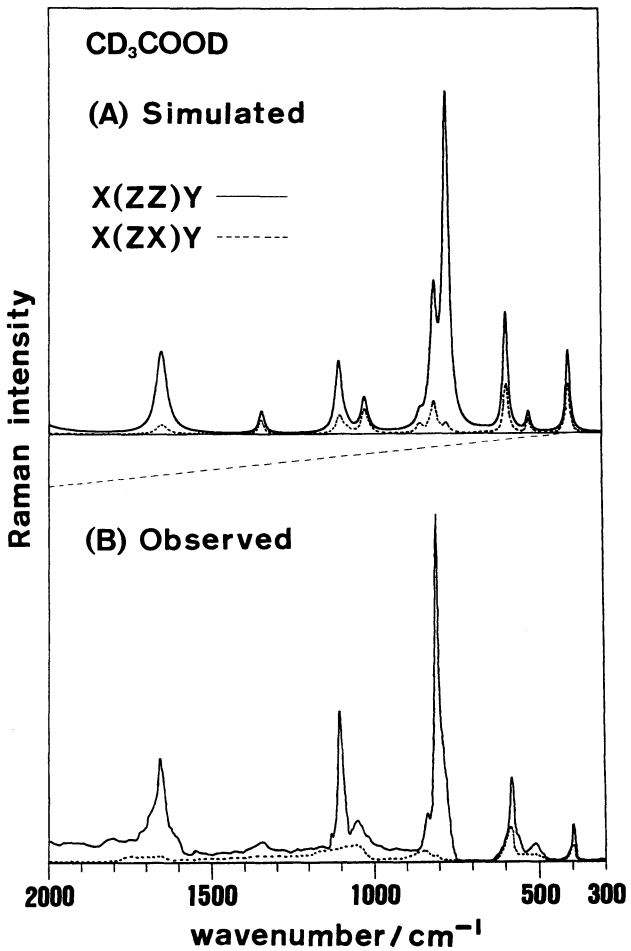

Fig. 5. Polarized Raman spectra of liquid perdeuterated acetic acid: (A) Simulated (ω_0=12 cm^{-1}) and (B) Observed. The experimental conditions, see caption of Fig. 1. For the frequency-dependent sensitivity correction, see caption of Fig. 4. The scattering geometry is X(Z,Z)Y (solid line) and X(Z,X)Y (dotted line).

few bands. The band widths, the Raman intensities, and the depolarization ratios were well simulated as compared with those observed. Furthermore, deuteration effects of the frequencies and the intensities are in reasonable agreement with the experiment. Extension of the present result to the molecular mechanical simulation of vibrational spectra of longer fatty acids, for which the double proton transfer within the dimeric ring raises complicated problems, is now in progress.

This work was supported by a Grand-in-Aid for Scientific Research No. 62570964 from the Ministry of Education, Science and Culture. The numerical calculations were carried out on FACOM M-780 computer system at the Data processing Center of Kyoto University.

References

1) R. C. Millikan and K. S. Pitzer, *J. Am. Chem. Soc.*, **80**, 3515 (1958).
2) P. Excoffon and Y. Maréchal, *Spectrochim. Acta, Part A*, **28**, 269 (1972).
3) J. Bournay and Y. Maréchal, *Spectrochim. Acta, Part A*, **31**, 1351 (1975).
4) a) I. Yokoyama, Y. Miwa, and K. Machida, *J. Am. Chem. Soc.*, **113**, 6458 (1991). b) I. Yokoyama, Y. Miwa, and K. Machida, *J. Phys. Chem.*, **95**, 9740 (1991).
5) a) K. Machida, H. Noma, and Y. Miwa, *Indian J. Pure Appl. Phys.*, **26**, 197 (1988). b) Y. Miwa and K. Machida, *J. Am. Chem. Soc.*, **110**, 5183 (1988); **111**, 7733 (1989).
6) J. B. Pedley, R. D. Naylor, and S. P. Kirby, "Thermochemical Data of Organic Compounds," 2nd ed, Chapman and Hall, London (1986).
7) A. D. H. Clague and H. J. Bernstein, *Spectrochim. Acta, Part A*, **25**, 593 (1969).
8) G. Henderson, *J. Chem. Educ.*, **64**, 88 (1987).
9) B. P. van Eijck, J. van Opheusden, M. M. M. van Schaik, and E. van Zoeren, *J. Mol. Spectrosc.*, **86**, 465 (1981).
10) J. L. Derissen, *J. Mol. Struct.*, **7**, 67 (1971).
11) S. Kishida and K. Nakamoto, *J. Chem. Phys.*, **41**, 1558 (1964).
12) M. Haurie and A. Novak, *J. Chim. Phys.*, **62**, 146 (1965).
13) W. Weltner, Jr., *J. Am. Chem. Soc.*, **77**, 3941 (1955).
14) J. K. Wilmshurst, *J. Chem. Phys.*, **6**, 1171 (1956).
15) M. Haurie and A. Novak, *J. Chim. Phys.*, **62**, 137 (1965).
16) C. V. Bernay, R. L. Redington, and K. C. Lin, *J. Chem. Phys.*, **53**, 1713 (1970).
17) H. R. Zelsmann, Z. Mielke, and Y. Maréchal, *J. Mol. Struct.*, **237**, 273 (1990).
18) O. F. Nielsen and P. A. Lund, *J. Chem. Phys.*, **78**, 652 (1983).
19) L. C. Krisher and E. Saegebarth, *J. Chem. Phys.*, **54**, 4553 (1971).
20) L. Pauling, "The Nature of the Chemical Bond," Cornell University, Ithaca, New York (1960).
21) H. Kim, R. Keller, and W. D. Gwinn, *J. Chem. Phys.*, **37**, 2748 (1962).
22) O. L. Stiefvater, *J. Chem. Phys.*, **62**, 233 (1975).
23) M. Gussoni, S. Abbate, and G. Zerbi, *J. Raman Spectrosc.*, **6**, 289 (1977).
24) S. Abbate, M. Gussoni, and G. Zerbi, *Indian J. Pure Appl. Phys.*, **16**, 199 (1978).
25) M. Gussoni, "Vibrational Intensities in Infrared and Raman Spectroscopy," ed by W. B. Person and G. Zerbi, Elsevier, Amsterdam (1982), Chap. 11, pp. 221—238.
26) C. H. Rhee, R. M. Metzger, and F. M. Wiygul, *J. Chem. Phys.*, **77**, 899 (1982).
27) E. R. Lippincott, G. Nagarajan, and J. M. Stutman, *J. Phys. Chem.*, **70**, 78 (1966).
28) R. G. Snyder, *J. Mol. Spectrosc.*, **36**, 204 (1970).
29) H. Noma, Y. Miwa, I. Yokoyama, and K. Machida, *J. Mol. Struct.*, **242**, 207 (1991).
30) D. R. Stull, E. F. Westrum, Jr., and G. C. Sinke, "The Chemical Thermodynamics of Organic Compounds," Wiley, New York (1969).
31) N. Lumbroso-Bader, C. Coupry, D. Baron, D. H. Clague, and G. Govil, *J. Magn. Reson.*, **17**, 386 (1975).
32) M. Perricaudet and A. Pullman, *Int. J. Peptide Protein Res.*, **5**, 99 (1973).
33) R. Meyer, T. Ha, H. Frei, and H. H. Günthard, *Chem. Phys.*, **9**, 393 (1975).
34) B. Crawford, Jr., *J. Chem. Phys.*, **29**, 1042 (1958).
35) Y. Maréchal, *J. Chem. Phys.*, **87**, 6344 (1987).
36) R. J. Jakobsen, Y. Mikawa, and J. W. Brasch, *Spectrochim. Acta, Part A*, **23**, 2199 (1967).
37) K. Fukushima and B. J. Zwolinski, *J. Chem. Phys.*, **50**, 737 (1969).
38) G. L. Carlson, R. E. Witkowski, and W. G. Fateley, *Spectrochim. Acta*, **22**, 1117 (1966).
39) J. E. Bertie and K. H. Michaelian, *J. Chem. Phys.*, **77**, 5267 (1982).
40) J. E. Bertie, H. H. Eysel, D. N. S. Permann, and D. H. Kalantar, *J. Raman Spectrosc.*, **16**, 137 (1985).
41) K. Nakamoto and S. Kishida, *J. Chem. Phys.*, **41**, 1554 (1964).
42) Y. Maréchal, "Molecular Interactions," ed by H. Ratajczak and W. J. Orville-Thomas, Wiley, New York (1980), Vol. 1, Chap. 8, pp. 231—272.
43) Y. Maréchal, *Can. J. Chem.*, **63**, 1684 (1985).
44) Y. Maréchal, "Vibrational Spectra and Structure," ed by J. Durig, Elsevier, Amsterdam (1987), Vol. 16, Chap. 5, pp. 311—356.
45) S. Bratos, J. Lascombe, and A. Novak, "Molecular Interactions," ed by H. Ratajczak and W. J. Orville-Thomas, Wiley, New York (1980), Vol. 1, Chap. 10, pp. 301—346.
46) S. R. Polo and M. K. Wilson, *J. Chem. Phys.*, **23**, 2376 (1955).
47) M. Akiyama, *J. Chem. Phys.*, **81**, 5229 (1984).
48) M. Akiyama, *J. Chem. Phys.*, **85**, 7 (1986).
49) H. Bertagnolli, *Chem. Phys. Lett.*, **93**, 287 (1982).